

# Manganese-diffusion-induced n-doping in semiconductor structures containing Ga(Mn)As layers

T. KORN<sup>1</sup>, R. SCHULZ<sup>1</sup>, S. FEHRINGER<sup>1</sup>, U. WURSTBAUER<sup>1</sup>, D. SCHUH<sup>1</sup>, W. WEGSCHEIDER<sup>1</sup>, M. W. WU<sup>2</sup> and C. SCHÜLLER<sup>1</sup>

<sup>1</sup> *Institut für Experimentelle und Angewandte Physik, Universität Regensburg, D-93040 Regensburg, Germany*

<sup>2</sup> *Hefei National Laboratory for Physical Sciences at Microscale and Department of Physics, University of Science and Technology of China, Hefei, Anhui, 230026, China*

PACS 73.61.Ey – Electrical properties of specific thin films - III V semiconductors

PACS 78.47.Cd – Time resolved luminescence

**Abstract.** - Semiconductor structures using ferromagnetic semiconductors as spin injectors are promising systems for future spintronic devices. Here, we present combined photoluminescence (PL) and time-resolved magneto-optical experiments of nominally nonmagnetic quantum wells (QWs) separated by a thin barrier from a ferromagnetic Ga(Mn)As layer. Due to the partial quenching of the PL, we conclude that there is a significant Mn backdiffusion into the QW. Moreover, from the time-resolved measurements, we infer that the Mn leads to n-type doping within the QW, and, in addition, strongly increases the electron spin dephasing time. The amount of Mn backdiffusion strongly depends on the barrier composition.

One key requirement for the development of semiconductor spintronic devices is the reliable injection of spin-polarized carriers into a nonmagnetic semiconductor structure [1, 2]. Here, ferromagnetic semiconductors like Ga(Mn)As [3] have emerged as an alternative to metallic ferromagnets. Highly efficient spin injection from Ga(Mn)As into a nonmagnetic heterostructure was demonstrated using a spin-LED structure [4]. Additionally, heterostructures using Ga(Mn)As show new magnetotransport phenomena, both tunneling anisotropic magnetoresistance (TAMR) [5], where a single ferromagnetic layer produces a spin-valve-like signal, and large-amplitude tunneling magnetoresistance (TMR) [6]. In the TMR structures, a thin (2 nm) GaAs layer between two Ga(Mn)As layers serves as a tunnel barrier.

In order to grow ferromagnetic Ga(Mn)As layers by molecular beam epitaxy (MBE), very low growth temperatures have to be used to inhibit Mn diffusion and MnAs formation. Due to the strong diffusion and segregation of Mn, it is expected that in any semiconductor structure containing a Ga(Mn)As layer, Mn will also be incorporated above and below the Ga(Mn)As. This is likely to cause background doping and strongly influences the transport properties of adjacent layers. Due to the close proximity of the p-metallic Ga(Mn)As, however, it is impossible to independently determine the type and concen-

tration of this background doping by transport measurements.

Here, we investigate this background doping by time- and spectrally-resolved optical techniques using a model system, which represents the combination of a ferromagnetic semiconductor and a two-dimensional structure. The combined analysis of time-resolved photoluminescence (TRPL) and time-resolved Faraday/Kerr rotation (TRFR/TRKR) experiments allows us to draw the conclusion that in our structures Mn diffusion leads to an n-type doping.

Our sample structure consists of two nominally undoped GaAs/Al<sub>0.3</sub>Ga<sub>0.7</sub>As quantum wells (QW) of different width, grown on a [001] GaAs substrate at the typical growth temperature of 600°C. The narrower QW (10 nm, here referred to as ref. QW) is grown first and serves as a reference. It is well-separated from the structures above by a 100 nm Al<sub>0.3</sub>Ga<sub>0.7</sub>As barrier. The wider QW (12 nm, here called Mn QW) is separated by a thin barrier from the 50 nm thick Ga(Mn)As layer, which is grown last at low temperature (250°C). Both, the QWs and the barrier are grown in the high-mobility chamber of a two-chamber MBE system (capable of achieving two-dimensional electron system mobilities well above 10<sup>7</sup> cm<sup>2</sup>/Vs). The sample is then transferred in vacuum to the second chamber, where the Ga(Mn)As layer is grown. Note that this sam-

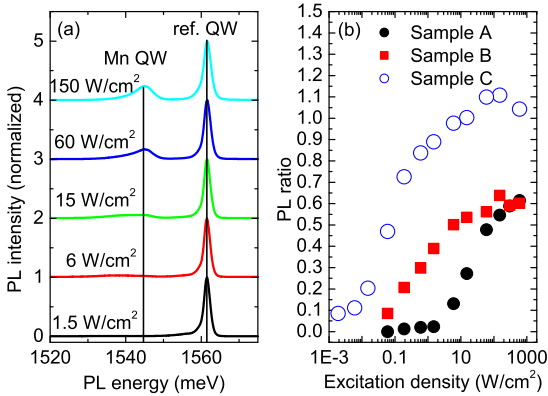


Fig. 1: (a) PL traces for the two QWs for different excitation densities, measured on sample A. (b) ratio of the PL peak areas for the two QWs as a function of excitation density. Black dots indicate sample A, red squares sample B, and blue open circles sample C.

ple design is different from systems studied by Poggio *et al.*, where Mn was directly incorporated into a QW during growth, causing incorporation of Mn on Ga sites [7]. Here, we present results from three samples with different barrier thickness and composition. Samples A and B: 4.34 nm of Al<sub>0.3</sub>Ga<sub>0.7</sub>As is grown on top of the QW layer. Then five periods of 3 monolayers (ML) AlAs / 1 ML GaAs are grown without rotation of the wafer, resulting in a total barrier thickness of 8.8 nm (sample A) and 11.1 nm (sample B). All layers are grown at 600°C. Sample C: 5 nm of Al<sub>0.3</sub>Ga<sub>0.7</sub>As is grown on top of the QW at 600°C, followed by 5 nm of Al<sub>0.8</sub>Ga<sub>0.2</sub>As grown at 250°C. We note that in all three samples, the total barrier thickness is significantly larger than in TMR structures based on Ga(Mn)As/GaAs.

We first study the photoluminescence (PL) of these samples as a function of excitation density, using a green (532 nm) cw laser. Figure 1 (a) shows typical PL spectra of sample A measured at 4 K. For low excitation density, only the PL of the ref. QW is visible. As the excitation density is increased, a PL signal from the Mn QW appears, but comparison between the PL lineshapes shows a significant broadening, and a pronounced low-energy shoulder in the emission from the Mn QW. In a reference sample grown in the same manner, but with the top layer consisting of low-temperature-grown GaAs without any Mn content, both QWs show essentially the same PL linewidth. As in a previous study [8], where we investigated different barrier widths, grown at high temperatures, we attribute this broadening and the quenching at low excitation density to Mn backdiffusion into the QW during growth of the Ga(Mn)As layer. In the QW, Mn ions act as centers for nonradiative recombination and partially quench the PL. Additionally, they also allow for the formation of bound excitons, which are redshifted by the additional binding energy. The observation of the broad low-energy shoulder in the PL spectrum, instead of a peak at low energy corre-

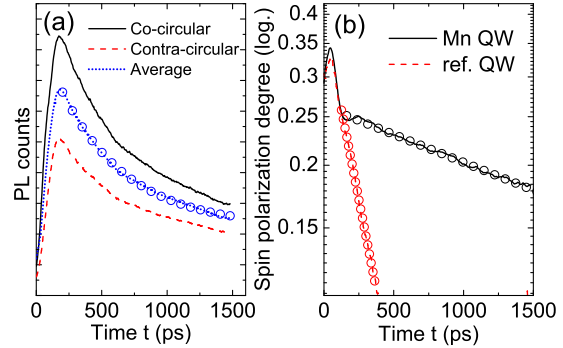


Fig. 2: (a) TRPL traces of the Mn QW in sample A for co- and contracircular configuration. The dotted line is the average of both. (b) Spin polarization degree traces for Mn and ref. QW in sample A. Open circles in both panels indicate exponential fits to the data.

sponding to a well-defined bound exciton state, indicates a large inhomogeneity of the bound states. Sample B and C show the same behavior, however, the PL from the Mn QW appears at lower excitation density. In Figure 1 (b), we show the ratio of the PL intensities of the Mn QW and the ref. QW, calculated from the peak areas, for all three samples. It is clearly visible how the PL from the Mn QW appears at a threshold excitation power and then saturates as the excitation power is increased further. In samples A and B, it only reaches about 60 percent of the ref. QW intensity, while in sample C both QWs have comparable PL intensity at high excitation. This behavior indicates that the nonradiative recombination centers are saturated as the density of photocarriers is increased. The different threshold powers of the three samples show that Mn diffusion depends strongly on the barrier thickness, and that a high Al content/low temperature-grown barrier is significantly more efficient at suppressing Mn diffusion than a superlattice. In order to observe the influence of Mn on the spin dynamics in the QW, we mainly focus on sample A, where the effects are more pronounced due to the largest Mn content.

We next discuss TRPL measurements performed at 4 K. Here, the sample is nonresonantly excited by circularly polarized 600 fs pulses from a modelocked Ti:sapphire laser. The circular polarization degree of the resulting PL is analyzed by a quarter-wave-plate and a polarizer. The PL is then detected by a streak camera system. Both, the recombination dynamics of the photocarriers in either QW, and their spin dynamics can be extracted from the TRPL traces. In subsequent measurements, first the TRPL with the same helicity (co-circular) as the excitation laser is recorded, then the TRPL with the opposite helicity (contra-circular). Figure 2(a) shows two time traces generated from TRPL data by averaging over a spectral window of 10 meV width around the spectral peak of the Mn QW. It is clearly visible that the co-circular TRPL is stronger than the contra-circular trace in the whole time window, indicating a finite spin polarization of the photo-

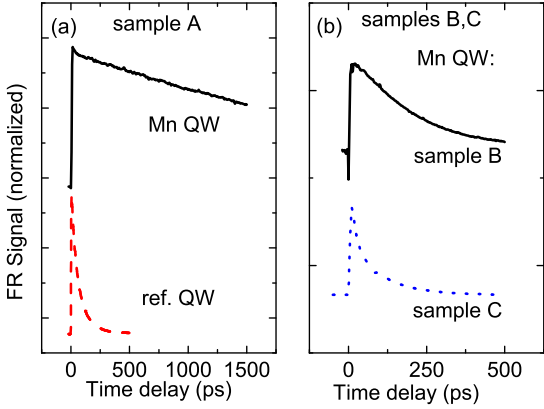


Fig. 3: (a) TRFR traces of the Mn QW (black solid line) and the ref. QW (red dashed line) in sample A, taken at zero magnetic field. (b) TRFR traces of the Mn QWs in samples B (black solid line) and C (blue dotted line), taken at zero magnetic field. Note the different time scales in (a) and (b).

carriers. The dotted line between the traces corresponds to the average of the traces. This reflects the recombination dynamics of the photocarriers. After a pronounced maximum of the TRPL, it decays exponentially with a time constant of 490 ps. For the ref. QW, a similar decay constant of the TRPL is found. The spin polarization degree (SPD) of the TRPL is calculated as follows: the difference between the co- and contra-circular traces is divided by their sum. Figure 2(b) shows the SPD of the Mn and the ref. QWs as a function of time on a logarithmic scale. While in the ref. QW, the SPD decays more quickly than the TRPL (313 ps decay time), we observe a significantly longer SPD decay in the Mn QW (3900 ps). One explanation for this drastic increase in spin dephasing time is motional narrowing: in one regime of the D’Yakonov-Perel spin dephasing mechanism [9], which is dominant in GaAs heterostructures at low temperatures, the spin dephasing time is inversely proportional to the momentum relaxation time. In the Mn QW, the Mn ions are efficient momentum scattering sites, leading to shorter momentum relaxation time than in the ref. QW. Although electron scattering at paramagnetic impurities like Mn allows for electron spin flips, at low impurity density motional narrowing dominates [10]. Additionally, electron localization at defects may also contribute to the increased spin dephasing time.

We further investigate this increase in spin dephasing time by performing TRFR/TRKR measurements. Both are two-beam pump-probe techniques: a circularly-polarized pump pulse from a mode-locked Ti:Sapphire laser is used for near-resonant excitation of either the Mn or the ref. QW. The spin polarization in the QWs is then detected by a second, time-delayed probe pulse from the same laser. This probe pulse is linearly polarized. Its polarization plane is rotated by a small angle proportional to the spin polarization, due to the Faraday (transmission)

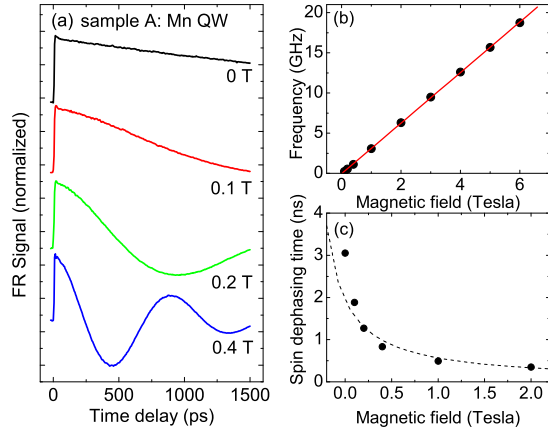


Fig. 4: (a) TRFR traces of the Mn QW in sample A for different applied in-plane magnetic fields. (b) Spin precession frequency for different in-plane magnetic fields measured for the Mn QW in sample A. The red line represents a linear fit. (c) Spin dephasing time of the Mn QW in sample A as a function of magnetic field. The dotted line represents a  $1/B$  dependence.

or Kerr (reflection) effects. This rotation angle is analyzed by an optical bridge detector. By scanning the delay between pump and probe pulses, the time dependence of the spin polarization is tracked. For measurements in transmission, the samples are glued to a transparent sapphire substrate, and the wafer side of the samples is removed by mechanical grinding and wet chemical etching, leaving only the MBE-grown layers.

Some differences between TRPL and TRFR/TRKR measurements need to be noted: in TRPL, nonresonant excitation is used, and spin information can only be extracted from the sample during the duration of the PL. Due to the selection rules in a GaAs QW and the fact that holes typically lose their spin orientation within a few ps [11], the circular polarization of the PL arises from the recombination of spin-polarized electrons. However, the spin polarization degree of the PL does not reflect the absolute spin polarization within the sample, which may change considerably due to carrier recombination: If we consider an undoped sample in which there is no electron spin relaxation, the TRPL spin polarization degree may remain constant during the duration of the PL, while the spin polarization in the sample decreases to zero as the photocarriers recombine. In TRFR/TRKR, resonant excitation is used to selectively excite one of the QWs, and the Faraday/Kerr rotation (FR/KR) signal is proportional to the absolute spin polarization within the QW. This spin polarization may arise from photocarriers, resident electrons or holes, or even localized moments due to magnetic impurities. Therefore, if there is a coherent spin polarization of resident carriers in the QW due to background doping, even after photocarrier recombination, a finite signal is measured.

Figure 3(a) shows TRFR traces taken at 4 K, where the laser was tuned to be resonant with the ground-state

transitions of either the Mn or the ref. QW in sample A. Under these excitation conditions, the photocarrier recombination time is typically much faster than for non-resonant excitation [12]. We observe a fast decay of the spin polarization for the ref. QW in sample A of about 100 ps, reflecting the photocarrier lifetime in the nominally undoped structure. Similar results are seen for the ref. QWs in all three samples. For the Mn QW in sample A, we observe a significantly longer decay of about 3 ns, corresponding to the slow decay of the SPD observed in the TRPL measurements, and indicating that a resident spin polarization remains within the QW after photocarrier recombination. In sample B (see Figure 3(b)), the spin lifetime of the Mn QW (200 ps) is also longer than that of the ref. QW (100 ps), while for sample C we observe similar spin lifetimes for both, the Mn QW and the ref. QW. These observations correspond to the intensity-dependent PL data (Fig. 1 (b)), in which sample C showed the lowest threshold excitation density and therefore the lowest Mn content.

In order to identify the type of the resident carriers, we apply an in-plane magnetic field to induce spin precession. In Figure 4(a), we show TRFR traces of the Mn QW (sample A) for different in-plane magnetic fields. A damped oscillation is observed, and both, the frequency and the damping of the oscillation, increase with magnetic field. A damped cosine function is fitted to the data to extract the frequency and the damping constant. In figure 4(b), this frequency is plotted as a function of the magnetic field. A linear fit to this dependence yields the  $g$  factor,  $|g| = 0.225$ . This value is in good agreement with the electron  $g$  factor in QWs of similar width [13]. From this, we can identify the resident carriers in the QW as electrons. The presence of resident electrons in the QW indicates that the Mn ions, which diffuse from the Ga(Mn)As layer into the heterostructure during growth, are incorporated mostly as interstitials, where they act as double donors [14]. In figure 4(c) we plot the spin dephasing time as a function of the in-plane magnetic field. A strong  $1/B$ -like dependence is seen, indicated by the dotted line. This behavior is caused by an inhomogeneity  $\Delta g$  of the electron  $g$  factor within the sample. The likely cause for this strong inhomogeneity is electron localization at defects [15].

In conclusion, we have investigated the diffusion of Mn ions from ferromagnetic Ga(Mn)As layers into a nonmagnetic heterostructure by optical spectroscopy techniques. The combination of time-resolved photoluminescence and time-resolved Faraday rotation allows us to determine that the diffusing Mn ions are incorporated as interstitials, and therefore act as double donors, causing an n-doping of layers adjacent to Ga(Mn)As. Additionally, the presence of Mn ions strongly increases the electron spin lifetime in the heterostructure. The diffusion of Mn strongly depends on the barrier composition and thickness. It can be partially suppressed by using a low-temperature-grown barrier with high Al content. Support by the DFG via SPP 1285 and

SFB 689, by the Natural Science Foundation of China under Grant 10725417, and the Robert-Bosch-Stiftung is gratefully acknowledged.

## REFERENCES

- [1] I. Zutic, J. Fabian, and S. Das Sarma, *Rev. Mod. Phys.* **76**, 323 (2004).
- [2] J. Fabian, A. Matos-Abiague, C. Ertler, Peter Stano, I. Zutic, *acta physica slovacica* **57**, 565 (2007).
- [3] H. Ohno, A. Shen and F. Matsukura, A. Oiwa, A. Endo, S. Katsumoto, and Y. Iye, *Appl. Phys. Lett.* **69**, 363 (1996).
- [4] P. Van Dorpe, Z. Liu, W. Van Roy, V. F. Motsnyi, M. Sawicki, G. Borghs, and J. De Boeck, *Appl. Phys. Lett.* **84**, 3495 (2004).
- [5] C. Rüster, C. Gould, T. Jungwirth, J. Sinova, G. M. Schott, R. Giraud, K. Brunner, G. Schmidt, and L. W. Molenkamp, *Phys. Rev. Lett.* **94**, 027203 (2005).
- [6] C. Gould, C. Rüster, T. Jungwirth, E. Girgis, G. M. Schott, R. Giraud, K. Brunner, G. Schmidt, and L. W. Molenkamp, *Phys. Rev. Lett.* **93**, 117203 (2004).
- [7] M. Poggio, R. C. Myers, N. P. Stern, A. C. Gossard, and D. D. Awschalom, *Phys. Rev. B* **72**, 235313 (2005).
- [8] R. Schulz, T. Korn, D. Stich, U. Wurstbauer, D. Schuh, W. Wegscheider, C. Schüller, *Physica E* **40**, 2163 (2008).
- [9] M.I. D'yakonov, and V.I. Perel, *Sov. Phys. Solid State* **13**, 3023 (1972).
- [10] J. H. Jiang, Y. Zhou, T. Korn, C. Schüller, and M. W. Wu, unpublished.
- [11] T. C. Damen, L. Via, J. E. Cunningham, J. E. Shah, and L. J. Sham, *Phys. Rev. Lett.* **67**, 3432 (1991).
- [12] E. A. Zhukov, D. R. Yakovlev, M. Bayer, M. M. Glazov, E. L. Ivchenko, G. Karczewski, T. Wojtowicz, and J. Kossut, *Phys. Rev. B* **76**, 205310 (2007).
- [13] M. J. Snelling, G. P. Flinn, A. S. Plaut, R. T. Harley, A. C. Tropper, R. Eccleston, and C. C. Phillips, *Phys. Rev. B* **44**, 11345 (1991).
- [14] F. Máca, J. and Mašek, *Phys. Rev. B* **65**, 235209 (2002).
- [15] Z. Chen, S. G. Carter, R. Bratschitsch, P. Dawson, and S. T. Cundiff, *Nature Physics* **3**, 265 (2007).